Asian Journal of Water, Environment and Pollution, Vol. 19, No. 6 (2022), pp. 75-84.
DOI 10.3233/AJW220091

Optimisation of Defluoridation of Water by Zirconia Nanoparticles Using RSM

Poornima G. Hiremath*, Prashanth G.K.[1], Abdul Bais Kadli, Sheril Varghese and Vishnu V. Bhaskar

Department of Chemical Engineering, Siddaganga Institute of Technology, Tumakuru – 572103, Karnataka, India
[1]Department of Master of Computer Application, Siddaganga Institute of Technology, Tumakuru – 572103, Karnataka, India
✉ pgh@sit.ac.in

Received April 19, 2021; revised and accepted September 19, 2022

Abstract: In the present work, zirconia nanoparticles were investigated for the adsorption of fluoride from water. The effect of the factor variables viz., the effect of initial fluoride concentration, adsorbent dosage, pH, and contact time and their interactions on adsorption of fluoride ion were investigated by response surface methodology (RSM) based on central composite design (CCD). The maximum fluoride removal was around 95% at 7 pH, initial fluoride concentration of 10 ppm, adsorbent dosage of 12.5 g/L, and contact time at 105 min. To understand the adsorption mechanism of fluoride on to the nanoparticles, adsorption isotherms and adsorption kinetics were studied. The Langmuir isotherm adsorption model and pseudo-second-order kinetics model fitted well for the fluoride removal using zirconia nanoparticles. The nanoparticles were characterised before and after for their adsorption using X-ray diffraction (XRD), Fourier transform infrared (FTIR) spectroscopy and SEM analysis.

Key words: Defluoridation, zirconia, nanoparticles, RSM, CCD.

Introduction

Fluoride is the most electronegative and reactive element that is essential in small quantities for a human being while a higher concentration of the same may cause toxic effects, such as dental fluorosis and skeletal fluorosis (Davenport, 2020; Gupta et al., 2007, 2008; Hiremath et al., 2016; Kapp et al., 2005; Zohoori et al., 2017). According to WHO, the fluoride concentration in drinking water should be less than 1.5 ppm for good health of human beings (Kanduti et al., 2016).

Various technologies, such as precipitation, adsorption, ion exchange, membrane separation, electro dialysis, etc. have been widely used and evaluated for fluoride removal (Biswas et al., 2007; Menkouchi et al., 2007). Adsorption is the most efficient and easily applicable technology for small treatment systems (Manyangadze et al., 2020). The process of adsorption using activated alumina (Ghorai et al., 2005), calcite (Turner et al., 2005), bone char (Medellin-Castillo et al., 2007), zeolite (Shaobin et al., 2010), and other low-cost materials is often approached as an inexpensive method for the defluoridation of water (Raju et al., 2017; Rajkumar et al., 2019). Recently, several novel materials like amine grafted graphene oxide encapsulated chitosan hybrid beads, anatase titanium dioxide nano-powder loaded 3D printed model devise, nanosized cerium oxides impregnated porous polystyrene anion exchanger, hydrous CeO_2 polypyrrole nanocomposite has been developed for defluoridation of water (Chigondo et.al., 2021; Hao et al., 2021; Jeyaseelan et al., 2021; Patel et al., 2021). Various zirconium-containing materials are

*Corresponding Author

also being tried for fluoride removal from water due to their high fluoride affinity (Dongre et al., 2012; Dou et al., 2012).

In the present study, the synthesised zirconium nanoparticles were investigated for their fluoride adsorption behaviour. The adsorption parameters were optimised using central composite design (CCD) based on response surface methodology (RSM) (Hiremath et al., 2016; Myers et al., 2002). The isotherms and kinetics of the adsorption process were also studied. The mechanism of fluoride removal by the adsorbent was understood based on the SEM analysis, FTIR Spectroscopy and XRD analysis.

Experimental Procedure

Materials

All chemicals and reagents used for the defluoridation were of analytical grade. During the study synthetic samples of fluoride were used. The zirconium nanoparticles were synthesised as per the procedure followed in the previous study (Negahdary et al., 2016).

The fluoride ion concentration of the solution was analysed using the Mettler Toledo fluoride ion selective electrode (perfect ION^{TM} combined fluoride electrode make) and Mettler Toledo ion analyser (Seven Compact pH/ion meter S220 make).

Batch Adsorption Experiments

Batch studies on optimisation of pH, initial fluoride concentration, adsorbent dosage, and contact time were conducted. The experiments were performed in 250-mL polypropylene flasks at a temperature of 30°C. The feed solution was prepared by adding a known amount of adsorbent and these samples were shaken in a temperature-controlled shaker at a speed of 190 rpm for a known period. These samples were then filtered using a syringe filter, and a clear solution was obtained. This clear solution was analysed to determine the residual fluoride concentration with the use of a fluoride ion selective electrode. As the membrane comes in contact with a solution holding fluoride ions, a potential is developed across the membrane. This electrode potential is determined against a constant reference potential and depends on the number of free fluoride ions present in the solution.

The percentage adsorption was calculated using Eq. (1).

$$\% \text{ Adsorption} = \frac{(C_0 - C_e)}{C_0} \times 100 \qquad (1)$$

where C_0 and C_e (mg/L) indicate the concentrations of fluoride ions present initially and at equilibrium in the sample, respectively.

Experimental Design and Data Analysis

The optimisation of the four variables, namely, pH (4.0–10.0), initial fluoride concentration (2–10 mg/L), adsorbent dosage (5–20 g/L) and contact time (30–180 min) were conducted using CCD of RSM. The response function of interest was percentage adsorption (R1), which was approximated by a second-degree polynomial equation using the method of least squares. Design Expert Version 9.0.3.1 (Stat-Ease, MA) software was employed for the optimisation of the process variables and also to assess the effects and mutual interactions of each process variable. The design consisted of a total of 30 runs with six replicates. In the statistical calculations, the four-factors, the range and the levels used in the trial are provided in Table 1. Table 2 represents the experimental design matrix obtained from CCD along with the percentage adsorption of fluoride ions using zirconium nanoparticles.

Table 1: The experimental factors and levels for the CCD

Factor	*Low level*	*Medium level*	*High level*
Initial F-concentration, ppm	2	6	10
Adsorbent dosage, g/L	5	12.5	20
pH	4	7	10
Contact time, min	30	105	180

Characterisation of the Adsorbent

The characterisation of the adsorbent was done using FTIR (Spectrum Two^{TM} from PerkinElmer, USA) to study the functional groups present in the adsorbent before and after fluoride adsorption. The surface morphology of the samples was observed using a scanning electron microscope (SEM, Ultra55 FESEM model from Carl Zeiss). Zirconia nanoparticles were also characterized using XRD (Bruker D8 Advance) before and after adsorption.

Equilibrium Studies

Equilibrium studies provide us the data on the uptake capacity of the adsorbent under experimental conditions. It helps us to find the model that fits the experimental

Table 2: CCD matrix and the percentage fluoride adsorption using zirconia nanoparticles

Run	*Initial conc. ppm*	*Adsorbent dosage g/L*	*pH*	*Time, min*	*% Removal (R1)*
1	6	12.5	7	105	94.75
2	2	20	10	30	37.20
3	2	5	4	180	88.45
4	6	12.5	7	105	92.24
5	2	5	10	180	35.75
6	2	20	4	30	87.90
7	6	12.5	10	105	47.33
8	6	12.5	7	105	93.17
9	10	12.5	7	105	95.34
10	6	12.5	4	105	95.65
11	10	5	4	180	88.32
12	2	20	10	180	79.22
13	10	20	10	180	78.45
14	6	12.5	7	105	93.12
15	6	5	7	105	79.50
16	10	20	10	30	35.15
17	2	5	4	30	93.50
18	6	12.5	7	180	95.11
19	10	5	10	30	5.10
20	2	20	4	180	93.97
21	10	20	4	180	95.53
22	6	12.5	7	30	79.24
23	6	20	7	105	95.18
24	10	5	10	180	34.55
25	2	5	10	30	7.20
26	2	12.5	7	105	94.72
27	10	20	4	30	88.50
28	6	12.5	7	105	95.12
29	6	12.5	7	105	95.14
30	10	5	4	30	93.30

data very well. Four adsorption isotherm models viz., Langmuir, Freundlich, Dubinin-Radushkevich (D-R) and Temkin isotherm models were considered in the current study (Malgorzata et al., 2002; Tan et al., 2008). Adsorption isotherm experiments were carried out in 250-mL polypropylene flasks containing 50 mL of solution with a fixed adsorbent dosage of 1.0 g/100mL and pH 7. The initial fluoride concentration varied between 2 and 10 ppm. These flasks were agitated at 190 rpm and maintained at 30°C for 3 h. The solutions were filtered and analysed for the residual fluoride concentration which is the equilibrium concentration (C_e). The equilibrium adsorbent concentration (q_e) is then calculated using Eq. (2) (Tan et al., 2008).

$$q_e = \frac{(C_0 - C_e)}{C_0} \times 100 \quad (2)$$

where q_e is the amount of fluoride adsorbed per unit weight of the sorbent at equilibrium (mg/g), C_e is the equilibrium concentration of fluoride in solution (mg/L), V is the volume of the fluoride solution (L) and M is the mass of adsorbent (g).

Adsorption Kinetics

In the present study, four different models viz., first order, pseudo-second order, Elovich and Intraparticle diffusion were studied to understand the kinetics of fluoride adsorption onto the adsorbent (Chhipa et al., 2013; Tan et al., 2008). A total of 250-mL polypropylene flasks containing 50 mL of fluoride solution and a known amount of adsorbent were placed in a temperature-controlled rotary shaker maintained at a speed of 190 rpm. The fluoride concentration was analysed at regular time intervals.

Results and Discussion

Characterisation of the Adsorbent

The FTIR spectra of zirconium before and after fluoride sorption are shown in Figure 1. FTIR spectra recorded peaks at 3500 cm^{-1} which is due to the–OH stretching vibrations at 2850 cm^{-1} because of C–H stretching (Smith, 1998). At 1500 and 1600 cm^{-1}, peaks may be attributed to H–O–H bond bending and the peak at 1353 cm^{-1} before adsorption was due to the bending vibration of Zr–OH groups (Smith, 1998). At 525 cm^{-1}, the peak shows crystalline Zr–O bonds. Zr–F and F–Zr–F bonds stretching is seen at around 375-400 cm^{-1} and 250-300 cm-1, which cannot be seen in mid IR region (Shakshooki et al., 2014). There is a decrease in the intensity of the plot in the range of 3000 cm^{-1} to 1500 cm^{-1}. This may be due to the adsorption of fluoride in the spectra of Zirconia.

The crystal structure of synthesised ZrO_2 nanoparticles has been investigated by generating diffraction patterns, XRD, from the crystalline powder samples at ambient temperature in the 2θ range of 20°–70°. The sharp peaks were observed in the plot of XRD data, which is due to the crystalline nature of the particle. The highest peak at the 2θ value of Zirconia is about 28° which can be clearly seen in the Figure 2. No major changes can be seen on the adsorbent before and after adsorption. But there is a slight decrease in the intensity in the XRD pattern after adsorption, which may be due to the fluoride adsorption onto the Zirconia particle.

SEM analysis is done to analyse the morphology of the Zirconia nanoparticles. Before and after SEM images of Zirconia nanoparticles are shown in Figure 3a,b. It was found that the particle size of nanoparticles is in the range of 40-60 nm. It can also be seen that all the particles are spherical in shape. The difference in the SEM images before and after adsorption is less. This may be due to the adsorption of fluoride ions into the pores of Zirconia nanoparticles.

Final Equation in Terms of Actual Factors

The final equation obtained from statistical analysis in terms of actual factors and which can be used to make predictions about the response (percentage fluoride removal) for given levels of each factor is given in Eq. (3).

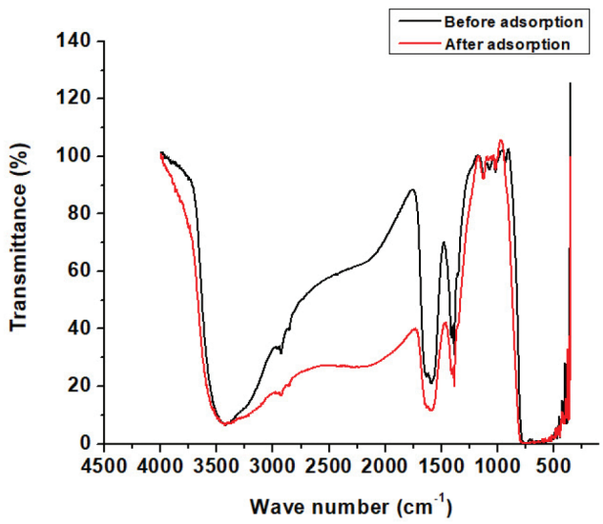

Figure 1: FT-IR of zirconium nanoparticles before adsorption and after adsorption.

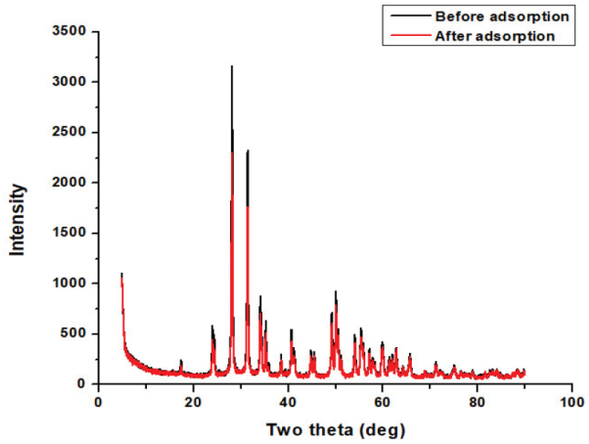

Figure 2: XRD of zirconium nanoparticles before adsorption and after adsorption.

R1 = 67.046 – (2.0590*Initial conc.) – (2.676*ads dose) + (16.745*pH) – (0.061*Contact time) + (0.062*Initial conc.*ads dose) – (0.0414*Initial conc.*pH) + ($6.687*10^{-4}$*Initial conc.*Contact time) + (4.253*ads dose*pH) + (0.0649*ads dose*Contact time) + (0.0412*pH*Contact time) + (0.179*Initial conc.^{2}) – (8.574*ads dose^2) – (2.519*pH^2) – ($8.867*10^{-4}$*Contact time^2) (3)

The empirical relationship between the response and process variables was obtained using one of the statistical testing tools called the F-test. The result of the analysis of variance (ANOVA) for the removal of fluoride ions is provided in detail in the Section Results and Discussion.

Validation of Response Surface Models and Statistical Analysis

ANOVA table for fluoride removal using zirconium nanoparticles indicates the importance of the individual factors and interactions between the parameters considered and the effect of parameters on the fluoride removal as represented in Table 3. Adsorbent dose, pH, contact time, and the square of pH were the factors that were found to be significant. The values of "Prob> F" (less than 0.0001) indicate that the terms are significant. Values above 0.1000 depict that the model terms are not significant. From Table 3, the lack-of-fit is found to be insignificant and proves that the obtained quadratic model is very much applicable to the study. Since the predicted R^2=0.9923 is almost nearer to the experimental R^2=0.9966, the experimental data fit well with the model. The real response data plotted against the predicted responses are shown in Figure 4 which depicts the actual versus predicted data were very close. The fluoride ion adsorption process was optimized using numerical optimization at a desirability value of 1.0. At the optimum conditions of initial concentration of 10 ppm, adsorbent dosage 12.5 g/L, pH 7 and contact time 105 minutes, the percentage removal was 94.79%. The experiments were conducted at the same optimum conditions and the percentage removal obtained was 95%. This confirms that the experimental results obtained were matching with that of the software.

Optimisation of Response Surfaces

The percentage of fluoride removal versus the effect of four factors (Effect of A: Initial fluoride concentration; B: Adsorbent dose; C: pH; D: contact time) can be

Table 3: ANOVA for the response of the percentage adsorption of fluoride ion onto zirconium nanoparticles

Source	*Sum of squares*	*df*	*Mean square*	*Value*	*PROB > F*	
Model	25553.19	14	1825.23	613.88	< 0.0001	Significant
A-Initial conc.	0.75	1	0.75	0.25	0.6232	
B-ads dose	1671.00	1	1671.00	562.01	< 0.0001	Significant
C-pH	13512.04	1	13512.0	4544.5	< 0.0001	Significant
D-Contact time	1610.47	1	1610.47	541.65	< 0.0001	Significant
AB	0.55	1	0.55	0.19	0.6729	
AC	3.95	1	3.95	1.33	0.2671	
AD	0.64	1	0.64	0.22	0.6483	
BC	1464.78	1	1464.78	492.65	< 0.0001	Significant
BD	213.53	1	213.53	71.82	< 0.0001	Significant
CD	1373.63	1	1373.63	462.00	< 0.0001	Significant
A^2	21.30	1	21.30	7.16	0.0173	
B^2	60.26	1	60.26	20.27	0.0004	
C^2	1331.87	1	1331.87	447.95	< 0.0001	Significant
D^2	64.46	1	64.46	21.68	0.0003	
Residual	44.60	15	2.97			
Lack of Fit	39.49	10	3.95	3.86	0.0744	Not significant
Pure Error	5.11	5	1.02			
Con Total	25597.79	29				

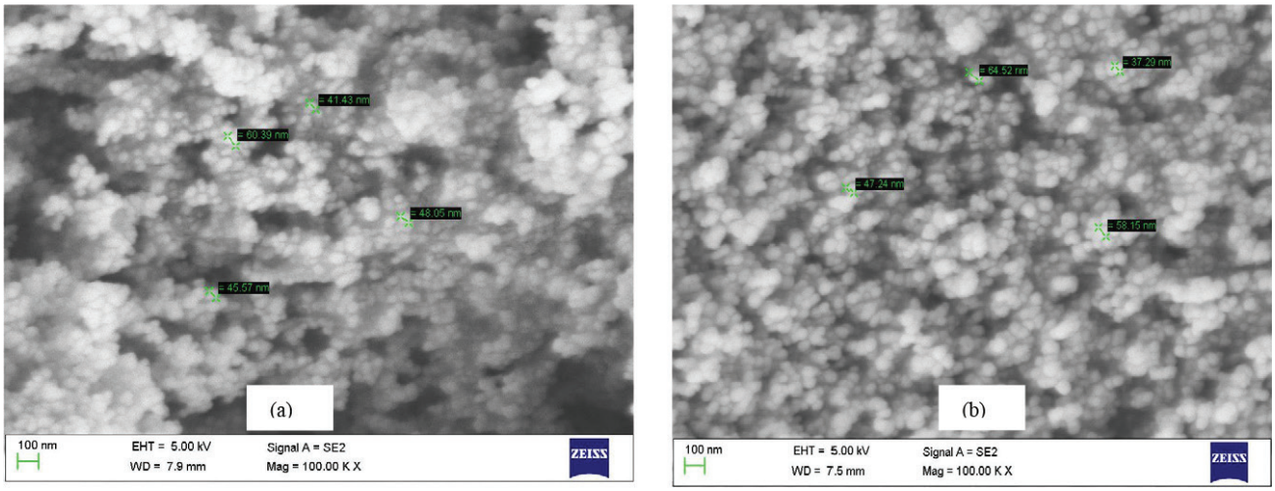

Figure 3: SEM images of zirconium (a) before adsorption and (b) after adsorption.

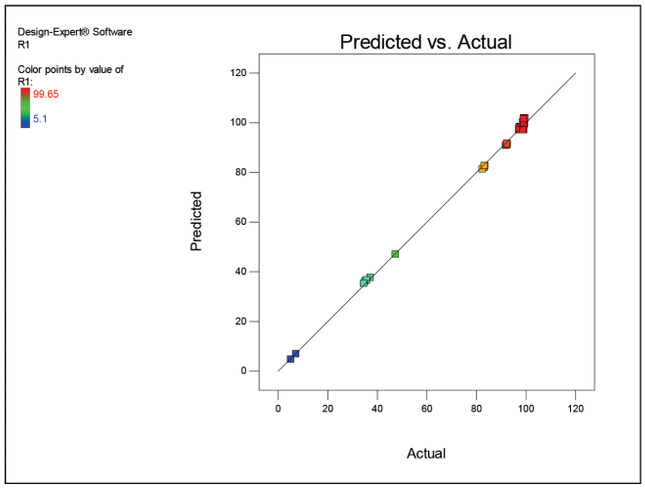

Figure 4: Predicted vs. actual response for adsorption of fluoride ions onto zirconium nanoparticles.

observed in Figure 5 (a-f). At higher pH, the fluoride removal efficiency was low maybe because of the competition between OH^- and F^- for adsorption and also due to the variations in the electrostatic force of attraction. At lower pH, protonation of the adsorbent surface is favoured giving rise to a greater number of positive sites per unit sorbent's surface area, further leading to higher adsorption. With the increase in the adsorbent dosage, fluoride removal is increased because of the higher surface area available for adsorption. Fluoride adsorption on Zirconia will take place until the equilibrium is reached i.e., 105 min, beyond which the extent of adsorption decreases. As the contact time increases, fluoride removal increases till it attains equilibrium condition. The removal of fluoride increases with an increase in the initial fluoride concentration as a greater number of fluoride ions will be competing to get adsorbed and occupy the vacant site of the adsorbent.

Adsorption Isotherm

Langmuir isotherm is found to fit the data well in a reasonable way with the highest regression coefficient value (R^2) of 0.9464 when compared to the other isotherm models as depicted in Figure 6 and Table 4. By spending the minimum energy, the utmost adsorption capacity was evident from the values of q_m and R_L values of 631.42 mg/g and 0.003 L/mg, respectively. The R_L value lies between 0 and 1 depicting that the adsorption is favourable and monolayer adsorption takes place. The Langmuir model assumes that adsorption occurs on a homogenous surface, where all adsorption sites are identical and energetically equivalent.

Adsorption Kinetics Studies

The mechanisms of adsorption were studied by using various kinetics models. Best fit was obtained in three kinetic models, namely, pseudo-second order adsorption, Elovich model, and Intraparticle model. Adsorption kinetic parameters for the fluoride removal by zirconium nanoparticles are provided in Table 5. Pseudo-second order adsorption assumes that adsorption takes place in two steps. The first step is faster and can attain equilibrium quickly and the second step is a lot slower process. Since the R^2 value is 0.999, the pseudo-second-order chemical reaction kinetics provides the best correlation of the experimental data over a long period (Figure 7). This model is based on the assumption that in all the systems studied the chemical reaction seems to be the significant rate-controlling step. It is assumed that due to chemisorption the fluoride ions

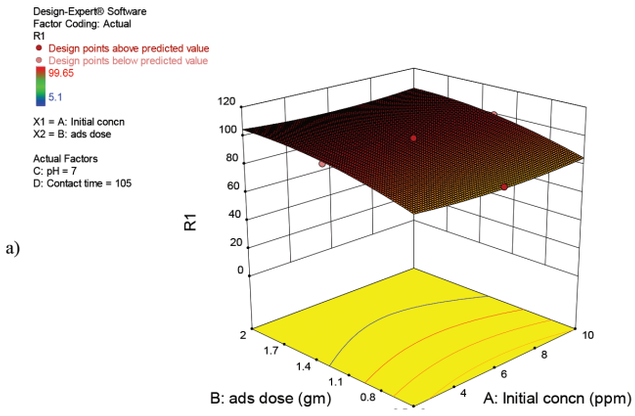

a)

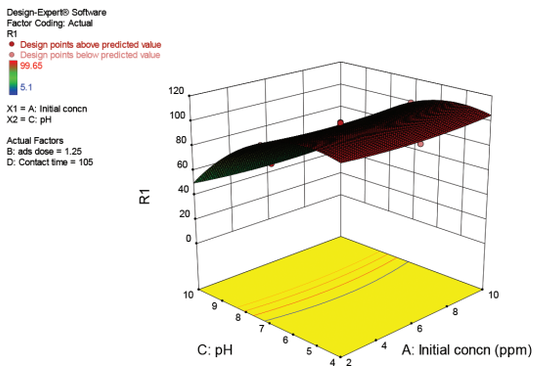

b)

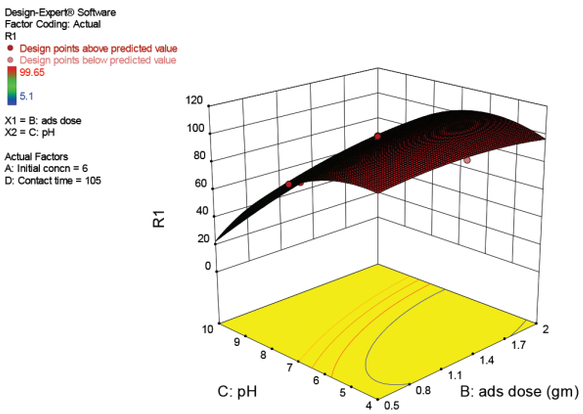

c)

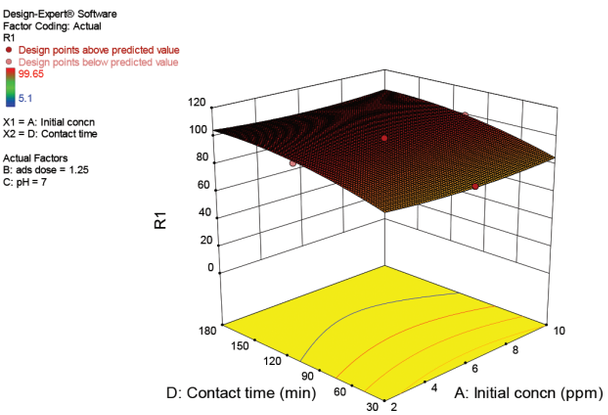

d)

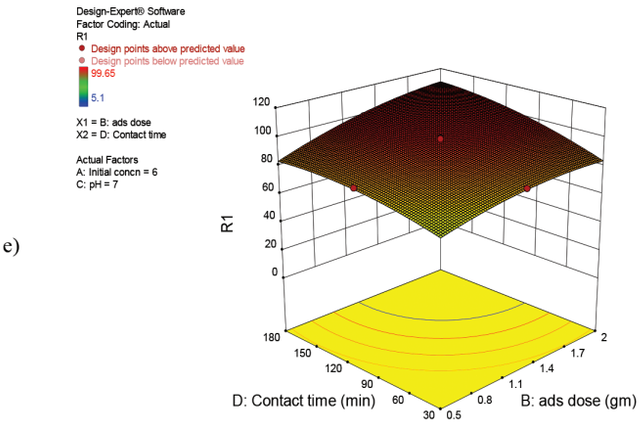

e)

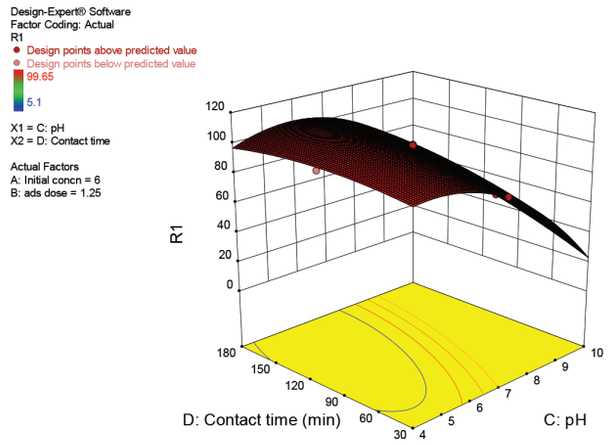

f)

Figure 5 (a-f): 3-D Response surface plots of percentage fluoride removal versus the effect of four variables (Effect of A: Initial fluoride concentration; B: Adsorbent dose; C: pH; D: contact time).

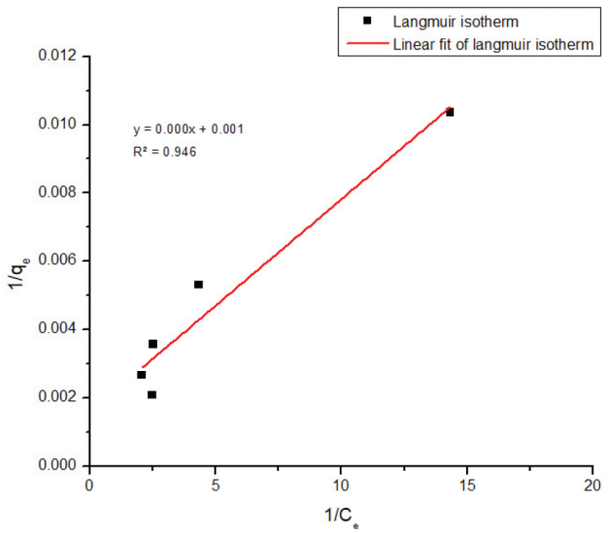

Figure 6: Langmuir isotherm of zirconium nanoparticles after adsorption.

Table 4: Adsorption isotherm parameters for the fluoride removal by zirconium nanoparticles

Isotherm	*Parameters*	*Value*	*Isotherm*	*Parameters*	*Value*
Langmuir	Slope: 1/ q_mK_a	0.0006	D-R	Slope: B_D	-4e-08
	Intercept: $1/q_m$	0.0016		Intercept: lnq_s	6.1612
	K_a (L/mg)	2.5381		B_D (mol^2/kJ^2)	0.0000
	q_m (mg/g)	631.4294		q_s (mg/g)	473.9905
	R_L	0.0039		E_D (kJ/mol)	3777.3451
	R^2	0.9464		R^2	0.8390
Freundlich	Slope: 1/n	0.7492	Temkin	Slope: B_T	159.5946
	Intercept: lnK_f	6.5119		Intercept: A_T(L/g)	497.7505
	N	1.3348		B_T	15.7827
	K_f (mg/g)	673.1219		A_T	3.1188
	R^2	0.8820		R^2	0.6982

Table 5: Adsorption kinetic parameters for the fluoride removal by zirconium nanoparticles

Kinetic model	*Parameters*	*Value*
First order	Slope	0.0111
	Intercept	0.0035
	q_1	3.1191
	R^2	0.8046
Pseudo second order	Slope	0.0034
	Intercept	0.0210
	R^2	**0.9992**
Elovich	Slope	25.1529
	Intercept	160.5730
	A	6.3839
	R^2	**0.9759**
Intraparticle	Slope	6.9415
	Intercept	203.9778
	R^2	**0.9780**

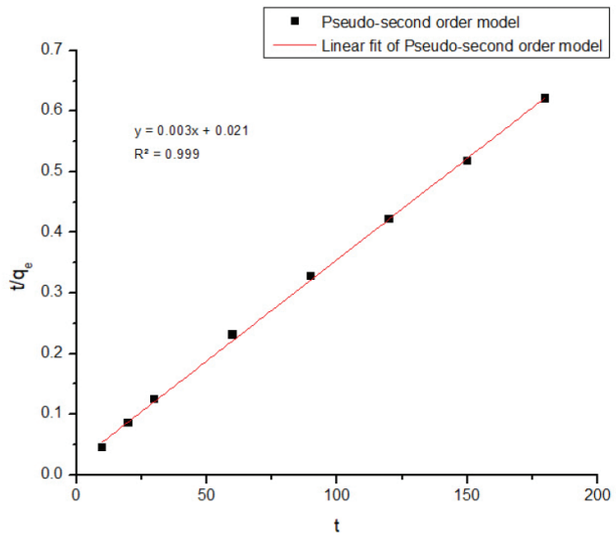

Figure 7: Pseudo-second order kinetic model of zirconium nanoparticles after adsorption.

form covalent bonds by sharing or exchange of electrons with the biosorbent surface and hence fluoride removal takes place.

Conclusion

The zirconium nanoparticles were used to remove fluoride from water. The FTIR spectroscopy, XRD and SEM studies proved that fluoride removal by this adsorbent occurred by the exchange of surface hydroxyl groups with fluoride, and by the electrostatic interaction between the charging surface and fluoride. RSM was used to optimise the factors influencing defluoridation. At pH 7.0, initial fluoride concentration 10 ppm, contact time 105 min and adsorbent dosage 12.5 g/L, the removal was found to be more than 95% using zirconium nanoparticles. From adsorption isotherm studies, the Langmuir isotherm model fitted the experimental data well. Therefore, it can be concluded that the adsorption of fluoride on Zirconia was due to monolayer adsorption. From kinetic studies, it was concluded that experimental data fitted very well with the pseudo-second order model. Hence, it is assumed that the rate-limiting step is chemisorption which involves the exchange of electrons between sorbent and sorbate.

References

Biswas, K., Bandhoyapadhyay, D. and U.C. Ghosh (2007). Adsorption kinetics of fluoride on iron(III)-zirconium(IV) hybrid oxide. *Adsorption*, **13:** 83-94.

Chigondo, M., Chigondo, F. and B. Nyamunda (2021). Synthesis of hydrous CeO_2 polypyrrole nanocomposite as a rapid and efficient adsorbent for defluoridation of drinking water. *Environmental Nanotechnology, Monitoring and Management*, **16:** 100462. https://doi.org/10.1016/j.enmm.2021.100462

Chhipa, H., Acharya, R., Bhatnagar, M. and A. Bhatnagar (2013). Determination of sorption potential of fermentation industry waste for fluoride removal. *International Journal of Bioassays*, **2:** 568-574.

Davenport, A. (2020). Chapter 44 - Trace Elements in Chronic Kidney Disease, in Chronic Renal Disease (Second Edition), Kimmel, P.L. and M.E. Rosenberg, Academic Press, pp. 703-717.

Dongre, R., Ghugal, D.N., Meshram, J.S. and D.S. Ramteke (2012). Fluoride removal from water by zirconium (IV) doped chitosan bio-composite. *African Journal of Environmental Science and Technology*, **6:** 130-141.

Dou, X., Mohan, D., Pittman, C.U. and S. Yang (2012). Remediating fluoride from water using hydrous zirconium oxide. *Chemical Engineering Journal*, **198-199:** 236-245.

Ghorai, S. and K.K. Pant (2005). Equilibrium, kinetics and breakthrough studies for adsorption of fluoride on activated alumina. *Separation and Purification Technology*, **42:** 265-271.

Gupta, P.K. (2018). Chapter 4 - Epidemiology of Animal Poisonings in Asia, in Veterinary Toxicology (Third Edition), R. C. Gupta, Ed., ed: Academic Press, pp. 57-69.

Gupta, V.K., Ali, I. and V.K. Saini (2007). Defluoridation of wastewaters using waste carbon slurry. *Water Research*, **41:** 3307-3316.

Hao, D., Huan, T., Xinxing, S., Wenlan, Y., Wenjing, C., Han, L., et al. (2021). Enhanced fluoride removal from water by nanosized cerium oxides impregnated porous polystyrene anion exchanger. *Chemosphere*, **287:** 131932, ISSN 0045-6535, https://doi.org/10.1016/j.chemosphere.2021.131932

Hiremath, P.G. and T. Theodore (2016). Modelling of fluoride sorption from aqueous solution using green algae impregnated with zirconium by response surface methodology. *Adsorption Science & Technology*, **35:** 194-217.

Jeyaseelan, A., Alsaiari, N.S., Katubi, K.M.M., Naushad, M. and N. Viswanathan (2021). Design and synthesis of amine grafted graphene oxide encapsulated chitosan hybrid beads for defluoridation of water. *International Journal of Biological Macromolecules*, **182:** 1843-1851. https://doi.org/10.1016/j.ijbiomac.2021.05.132

Kanduti, D., Sterbenk, P. and B. Artnik (2016). Fluoride: A review of use and effects on health. *Materia Socio-medica*, **28:** 133-137.

Kapp, R. (2005). Fluorine. *In:* Encyclopedia of Toxicology (Second Edition), Wexler, P., Ed., New York: *Elsevier*, pp. 343-346.

Malgorzata, B. (2002). Adsorption on heterogeneous surfaces, in Adsorption: Theory, Modeling and Analysis. *Toth, J.*, CRC Press, New York, NY, USA, **107:** 112-115.

Manyangadze, M., Chikuruwo, N.H.M., Narsaiah, T.B., Chakra, C.S., Radhakumari, M. and G. Danha (2020). Enhancing adsorption capacity of nano-adsorbents via surface modification: A review. *South African Journal of Chemical Engineering*, **31:** 25-32.

Medellin-Castillo, N.A., Leyva-Ramos, R., Ocampo-Perez, R., Garcia de la Cruz, R.F., et al. (2007). Adsorption of fluoride from water solution on bone char. *Industrial & Engineering Chemistry Research*, **46:** 9205-9212.

Menkouchi, M.A., Annouar, S., Tahaikt, M., Mountadar, M., Soufiane, A. and A. Elmidaoui (2007). Fluoride removal for underground brackish water by adsorption on the natural chitosan and by electrodialysis. *Desalination*, **212:** 37-45.

Myers, R.H. and D.C. Montgomery (2002). Response Surface Methodology, Wiley, New York.

Negahdary, M., Habibi-Tamijani, A., Asadi, A. and S. Ayati (2013). Synthesis of zirconia nanoparticles and their ameliorative roles as additives concrete structures. *Journal of Chemistry*, **2013:** 314862.

Patel, R.K., Chawla, A.K., Manna, S. and J.K. Pandey (2021). Defluoridation of water using anatase titanium dioxide nano-powder loaded 3D printed model devise. *Journal of Water Process Engineering*, **40:** 101785. https://doi.org/10.1016/j.jwpe.2020.101785

Rajkumar, S., Murugesh, S., Sivasankar, V., Darchen, A., Msagati, T.A.M. and T. Chaabane (2019). Low-cost fluoride adsorbents prepared from a renewable biowaste: Syntheses, characterization and modeling studies. *Arabian Journal of Chemistry*, **12**, pp. 3004-3017.

Raju, K.B.C., Reddy, D., Gayathri, G. and B. Matcha (2017). Defluoridation of ground water using low cost adsorbents. *International Journal of Earth Sciences and Engineering*, **10:** 967-972.

Shakshooki, S.K., Mohamed Hassan, B., EL-Nowely, K.W., ElBelazi, A., Abed, S.M. and M.M. Al-Said (2014). α-Zirconium titanium phosphates-fibrous cerium phosphate composite membranes and their 1, 10- Phenanthroline Cu(II) pillared materials. *Physics and Materials Chemistry*, **2:** 7-13.

Shaobin, W. and Y. Peng (2010). Natural zeolites as effective adsorbents in water and wastewater treatment. *Chemical Engineering Journal*, **156:** 11-24.

Smith, B.C. (1998). Infrared Spectral Interpretation: A Systematic Approach, 1st edition. CRC Press, London, UK.

Tan, I.A.W., Ahmad, A. and B.H. Hameed (2008). Adsorption of basic dye on high-surface-area activated carbon prepared from coconut husk: Equilibrium, kinetic and

thermodynamic studies. *Journal of Hazardous Materials*, **154:** 337-346.

Turner, B.D., Binning, P. and S.L.S. Stipp (2005). Fluoride removal by calcite: Evidence for fluorite precipitation and surface adsorption. *Environmental Science & Technology,* **39:** 9561-9568.

Zohoori, F.V. and R.M. Duckworth (2017). Fluoride: Intake and Metabolism, Therapeutic and Toxicological Consequences, in Molecular, Genetic, and Nutritional Aspects of Major and Trace Minerals, Chapter 44, Collins, J.F. (ed.). Boston: Academic Press, pp. 539-550.